Molecular Crystals and Liquid Crystals Incorporating Nonlinear Optics

Publication details, including instructions for authors and subscription information:
http://www.tandfonline.com/loi/gmcl17

Measurement of The Third Order Optical Susceptibility of Quasi-Two Dimensional Conjugated Discs: Silicon Naphthalocyanine

N. Q. Wang [a] , Y. M. Cai [a] , J. R. Heflin [a] & A. F. Garito [a]

[a] Department of Physics, University of Pennsylvania, Philadelphia, PA, 19104

Version of record first published: 22 Sep 2006.

To cite this article: N. Q. Wang , Y. M. Cai , J. R. Heflin & A. F. Garito (1990): Measurement of The Third Order Optical Susceptibility of Quasi-Two Dimensional Conjugated Discs: Silicon Naphthalocyanine, Molecular Crystals and Liquid Crystals Incorporating Nonlinear Optics, 189:1, 39-48

To link to this article: http://dx.doi.org/10.1080/00268949008037220

Mol. Cryst. Liq. Cryst., 1990, Vol. 189, pp. 39–48
Reprints available directly from the publisher
Photocopying permitted by license only

Printed in the United States of America

Measurement of The Third Order Optical Susceptibility of Quasi-Two Dimensional Conjugated Discs: Silicon Naphthalocyanine

N. Q. WANG, Y. M. CAI, J. R. HEFLIN and A. F. GARITO
Department of Physics, University of Pennsylvania, Philadelphia, PA 19104

The isotropically averaged nonresonant microscopic third order susceptibility $<\gamma>$ has been measured for a quasi-two dimensional metallophthalocyanine at several near infrared wavelengths. An infinite dilution extrapolation method employing the Maker fringe technique for third harmonic generation in the wedge configuration was developed for measurement of $<\gamma>$ in liquid solutions and is presented in detail. At a fundamental wavelength of 1907 nm, $<\gamma>$ of silicon naphthalocyanine is measured to be $-3140 \pm 250 \times 10^{-36}$ esu whereas $<\gamma>$ is less than the experimental sensitivity of $\pm 50 \times 10^{-36}$ esu for a fundamental wavelength of 1543 nm. These results are discussed in terms of the dispersion of $<\gamma>$ in the region between the 3ω resonances associated with the Q and B absorption bands.

1. INTRODUCTION

Conjugated π-electron organic and polymer structures are now well known to exhibit unusually large macroscopic second order, $\chi^{(2)}_{ijk}(-\omega_3;\omega_1,\omega_2)$, and third order, $\chi^{(3)}_{ijkl}(-\omega_4;\omega_1,\omega_2,\omega_3)$, nonlinear optical susceptibilities, and their microscopic origin and virtual excitation processes can be successfully described by many-electron theory of highly correlated quasi-one (1D) and two (2D) dimensional systems.[1–3] In the quasi-2D case of metallophthalocyanines,[4–10] studies of the resonant third order optical properties of disk-like silicon naphthalocyanine (SINC) (Figure 1), randomly dispersed in glassy polymer films, demonstrated that SINC behaves as an optical Bloch two level system, exhibiting absorption saturation of the large oscillator strength ($\alpha_0 = 1 \times 10^5$ cm^{-1}) Q band in the near infrared range (810 nm) and an associated, large, intensity dependent refractive index n_2 of 1×10^{-4} cm^2/KW.[5–7] These intrinsic properties are the basis for the first observation of absorptive optical bistability occurring through the nonlinear electronic excitations of a random solid medium. In this paper, our purpose is to extend our studies of

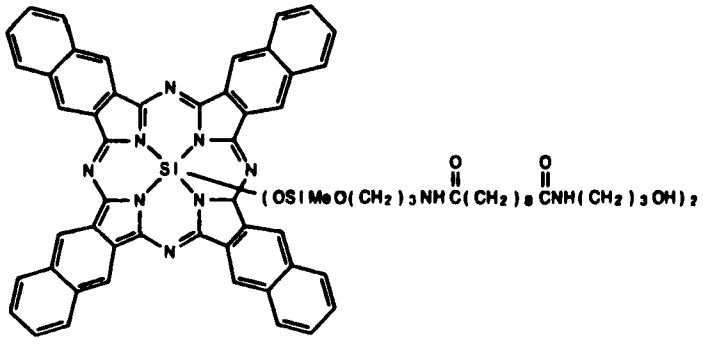

FIGURE 1 Schematic diagram for the molecular structure of silicon naphthalocyanine (SINC).

SINC to measurements of the nonresonant third order optical properties in the near infrared range of individual SINC molecules.

The important spectral features of the SINC films are essentially the same in liquid solution. As shown in Figure 2, SINC exhibits a characteristic, vibronically coupled, large oscillator strength Q band centered at 778 nm, and, after a relatively large transparent region (500 nm–600 nm), a B (Soret) band located near 335 nm. The Q and B bands are due to widely separated $S_0(1^1Ag) \rightarrow S_1(1^1Eu)$ and $S_0(1^1Ag) \rightarrow S_2(2^1Eu)$ π-electron transitions, respectively, as is well-established for metallophthalocyanines and related metalloporphyrins of D_{4h} symmetry.[11–13]

In the present paper, an infinite dilution extrapolation method is developed for liquid solution measurements of the isotropically averaged value $\langle\gamma\rangle$ of the molecular third harmonic susceptibility $\gamma_{ijkl}(-3\omega;\omega,\omega,\omega)$ based on the Maker fringe technique for third harmonic generation (THG) in the wedge configuration.[14] The

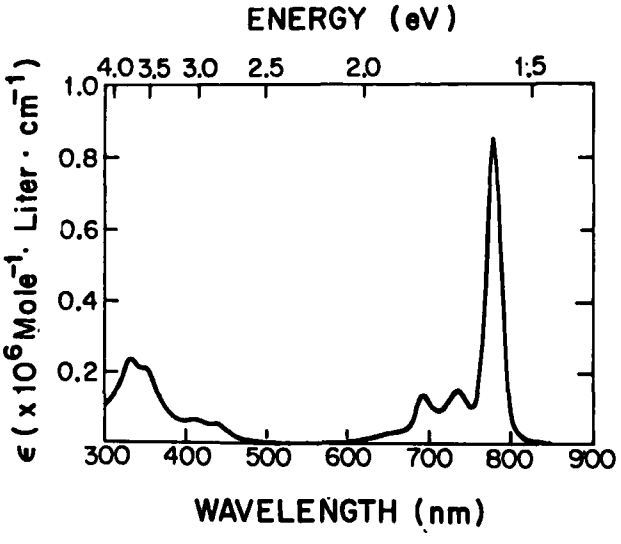

FIGURE 2 Linear absorption spectrum of SINC in DMF. The Q band absorption peak occurs at 778 nm (1.59 eV) and B band peak at 335 nm (3.70 eV). The solution is transparent between 500–600 nm.

dispersion of $<\gamma>$ for SINC dissolved in dimethyl formamide (DMF) is measured for 10 ns pulses at the fundamental wavelengths of 1907, 1543 and 1064 nm. At 1907 nm, the value of $<\gamma>$ for SINC is $-3140 \pm 250 \times 10^{-36}$ esu, and, at shorter wavelengths, $<\gamma>$ is immeasurably small, being less than the experimental uncertainty of $\pm 50 \times 10^{-36}$ esu at 1543 nm. After the infinite dilution analysis, these results are discussed in terms of the dispersion of $<\gamma>$ in the region between the 3ω resonances associated with the $S_0 \rightarrow S_1$ Q and $S_0 \rightarrow S_2$ B band excitations.

2. EXPERIMENT

The basic optical layout of sample and reference arms for the liquid solution THG measurements is similar to that described previously for DC induced second harmonic generation (DCSHG) measurements.[15-16] The laser source is a 10 Hz, 10 ns pulse width, Q-switched Nd:YAG laser with 120 mj/pulse maximum output at a fundamental wavelength of 1064 nm. The 1907 nm fundamental is generated through stimulated Raman scattering (SRS) by focusing the 1064 nm output into a hydrogen gas cell. To generate the 1543 nm fundamental, the hydrogen cell is replaced with a methane gas cell. In the sample arm, the fundamental beam is focussed on the sample cell containing a liquid solution of SINC dissolved in transparent DMF. The solutions were prepared under inert gas conditions and purged with nitrogen or argon for 15–30 minutes just prior to use.

The sample cell (Figure 3) consists of two 12.7 cm BK-7 glass windows mounted to form a 0.0223 rad wedge compartment with mean thickness 0.44 mm. The waist of the Gaussian beam is 70 μm at the center of the sample. At the two liquid- glass interfaces, the beam width is expanded no more than 0.1% such that the fundamental intensity remains essentially constant throughout the sample. At the two air-glass interfaces, however, the beam intensity is reduced by two orders of magnitude compared to the intensity in the liquid compartment, eliminating the contribution of $\chi^{(3)}$ from air at the air-glass boundaries. The sample cell is mounted on a computer-controlled, stepping motor driven translation stage where the translational axis is perpendicular to the direction of beam propagation. The third harmonic signal generated in the sample cell is measured as a function of beam

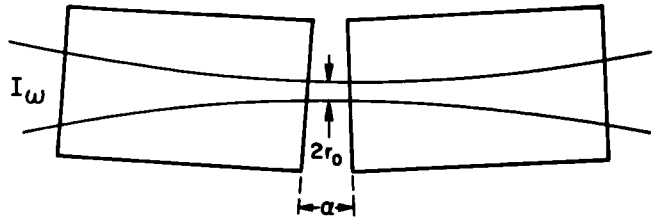

FIGURE 3 The THG sample cell design. The two BK-7 glass windows with dimensions 127 × 30 × 20 mm³. The sample compartment has an average thickness of 1 mm and a wedge angle α of 0.0223 rad. The weakly focused laser beam has a waist r_0 of 70 μm at the center of the sample and is expanded no more than 0.1% at the two sample-glass boundaries. The beam intensity is reduced by two orders of magnitude at the air-glass boundaries compared to at the center of the sample.

pathlength through the sample, and the third harmonic susceptibility $\chi^{(3)}(-3\omega;\omega,\omega,\omega)$ of the sample liquid is determined by calibrating the results against a solvent of known $\chi^{(3)}(-3\omega;\omega,\omega,\omega)$.

The fundamental beam is split into separate reference and sample arms. The purpose of the reference is to divide out any laser power fluctuations. THG signal from the sample cell is detected by PMT2. Since the ratio of the two outputs from PMT1 and PMT2 is independent of the fundamental input power, the effects due to fluctuations in the fundamental beam intensity were minimized. A PDP-11 lab computer was utilized for data acquisition and signal averaging through a CAMAC interface.[17]

3. ANALYSIS AND RESULTS

The weakly focused fundamental laser beam can be approximated as a plane wave in the sample region. Standard treatment involving free and bound waves was employed to derive an analytical expression for the third harmonic intensity of the sample. Since both the input and the output window surfaces are distant from the sample region of the weakly focused fundamental beam and the intensity is greatly reduced at these surfaces, only the glass-liquid (G-L) and liquid-glass (L-G) boundaries need to be considered in solving the boundary conditions for the wave equations. The THG intensity $I_{3\omega}$ is then given by the expression

$$I_{3\omega} = (96\pi/c^2)^2\omega^2(t_{3\omega}^G)^2(t_\omega^{(1)})^6(I_\omega)^3\left[T_G\frac{l_c^G\chi_G^{(3)}}{n_{3\omega}^G + n_\omega^G} - T_L\frac{l_c^L\chi_L^{(3)}}{n_{3\omega}^L + n_\omega^L}(t_\omega^{(2)})^3\right]^2 f(l) \quad (1)$$

where the transmittance factors t and T are

$$t_{3\omega}^G = \frac{2n_{3\omega}^G}{1 + n_{3\omega}^G},\ T_L = \frac{n_\omega^L + n_{3\omega}^L}{n_{3\omega}^G + n_{3\omega}^L},\ T_G = \frac{n_\omega^G + n_{3\omega}^L}{n_{3\omega}^G + n_{3\omega}^L},$$

$$t_\omega^{(1)} = \frac{2}{(1 + n_\omega^G)},\ t_\omega^{(2)} = \frac{2n_\omega^G}{(n_\omega^G + n_\omega^L)},$$

l_c is the coherence length

$$l_c = \frac{\pi c}{3\omega(n_{3\omega} - n_\omega)}, \quad (2)$$

and $f(l)$ is the interference term

$$f(l) = e^{-(3\alpha_\omega/2 + \alpha_{3\omega}/2)l}\{cosh[3\alpha_\omega/2 - \alpha_{3\omega}/2)l] - cos(\pi l/l_c^L)\} \quad (3)$$

where l is the sample thickness and α_ω and $\alpha_{3\omega}$ the linear absorptivity coefficients

at the fundamental (ω) and third harmonic (3ω) frequencies, respectively. In the absence of any absorption ($\alpha_\omega = \alpha_{3\omega} = 0$), $f(l)$ reduces to

$$f(l) = 2\sin^2\left(\frac{\pi l}{2l_c^L}\right) \tag{4}$$

which is the standard Maker fringe interference pattern. The average fundamental power was kept to less than 5 mJ/pulse, such that the laser intensity is below the damage thresholds of glass and the liquid solutions. $\chi^{(3)}(-3\omega;\omega,\omega,\omega)$ is obtained by fitting the third harmonic fringes to a function of the form

$$I_{3\omega} = A_1\sin^2\left(\frac{\pi l}{2A_3} + \frac{A_4}{2}\right) + A_2 \tag{5}$$

where A_1 is the fringe amplitude, A_2 is the minimum fringe height which can be nonzero due to finite beam size effects as well as absorption in the solution at either ω or 3ω photon energies, A_3 is the coherence length l_c, and A_4 is an arbitrary phase factor. It can be shown that the mean value of the fringes, $A_m = A_1/2 + A_2$, obeys the relation

$$\frac{(A_m^L)_{corr}}{A_m^R} = \frac{\left[T_G\dfrac{l_c^G\chi_G^{(3)}}{n_{3\omega}^G + n_\omega^G} - T_L\dfrac{l_c^L\chi_L^{(3)}}{n_{3\omega}^L + n_\omega^L}(t_\omega^{(2)})^3\right]^2}{\left[T_G\dfrac{l_c^G\chi_G^{(3)}}{n_{3\omega}^G + n_\omega^G} - T_R\dfrac{l_c^R\chi_R^{(3)}}{n_{3\omega}^R + n_\omega^R}(t_\omega^{(2)})^3\right]^2} \tag{6}$$

where

$$(A_m^L)_{corr} = \frac{2(A_m^L)_{obs}}{e^{-3\alpha_\omega l} + e^{-\alpha_{3\omega} l}} \tag{7}$$

is the mean value of the fringes of the liquid solution corrected for any absorption at ω and 3ω and R refers to the reference liquid.

The values of $\chi^{(3)}$ and l_c of BK-7 glass and DMF at 1907 nm fundamental were taken as $\chi_G^{(3)} = 4.67 \times 10^{-14}$ esu, $l_c^G = 16.7$ μm, $\chi_{DMF}^{(3)} = 5.05 \times 10^{-14}$ esu and $l_c^{DMF} = 22.41$ μm.[18,19] At $\lambda = 1543$ nm for BK-7 glass, the values for $\chi_G^{(3)}$ of 4.73×10^{-14} esu and for l_c^G of 13.03 μm were obtained from the dispersion relation for the refractive index of BK-7 and Miller's rule applied to $\chi_G^{(3)}$ at 1907 nm. For DMF at 1543 nm, we obtained the values for $\chi_{DMF}^{(3)}$ of 5.28×10^{-14} esu and for l_c^{DMF} of 14.3 ± 0.1 μm.

The concentration dependence of the solution $\chi_L^{(3)}$ at 1907 nm is shown in Figure 4. The values of $\chi_L^{(3)}$ decrease linearly with increased concentration of SINC, showing that the SINC contribution is negative in sign.

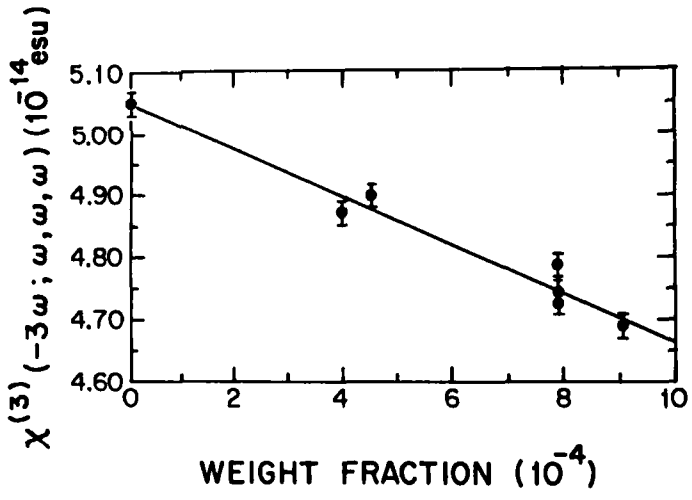

FIGURE 4 Concentration dependence of $\chi_L^{(3)}(-3\omega;\omega,\omega,\omega)$ for solutions of SINC in DMF at 1907 nm fundamental wavelength.

4. DISCUSSION

For a two-component system, the solution macroscopic $\chi_L^{(3)}$ is related to the microscopic susceptibilities γ_i of each component through

$$\begin{aligned}\chi_L^{(3)} &= N_1 f_{1\omega}^3 (f_1^\omega)^3 \gamma_1 + N_2 f_2^{3\omega} (f_2^\omega)^3 \gamma_2 \\ &= N_1 F_1 \gamma_1 + N_2 F_2 \gamma_2\end{aligned} \tag{8}$$

where $N_1(N_2)$ is the number density of the solute (solvent), and $f_1(f_2)$ is local the field factor of the solute (solvent). In order to account for local field effects and the solute-solute, and solvent-solvent interactions, we have extended the infinite dilution extrapolation method for DCSHG[15] to measurements of $\chi_L^{(3)}$. The method requires combined measurements of the concentration dependence of$\chi_L^{(3)}$ and the refractive index n.

The number densities N_1 and N_2 can be expressed as

$$N_1 = \frac{N_A W_1}{V M_1} \qquad N_2 = \frac{N_A W_2}{V M_2} \tag{9}$$

with $w = W_1/(W_1 + W_2)$ defined as the weight fraction of the solute, and $v = V/(W_1 + W_2)$ as the specific volume, then

$$N_1 = \frac{N_A w}{v M_1} \qquad N_2 = \frac{N_A (1 - w)}{v M_2} \tag{10}$$

and Equation (8) becomes

$$\chi_L^{(3)} = \frac{N_A w}{vM_1} F_1 \gamma_1 + \frac{N_A(1 - w)}{vM_2} F_2 \gamma_2. \tag{11}$$

For the local field factor f_i, we adopt the Lorenz-Lorentz model where the indices of refraction $n_{3\omega} \cong n_\omega = n$

$$f_i^{3\omega} = f_i^{\omega} = \frac{n^2 + 2}{3} \tag{12}$$

and

$$F_i = \left(\frac{n^2 + 2}{3}\right)^4 \tag{13}$$

where n is the refractive index of the solution.

Taking the derivative with respect to w on both sides of Equation (11) and extrapolating to infinite dilution where $w \to 0$, we obtain the following equation for determining the microscopic third-order susceptibility γ_1 of the solute

$$v_0 \frac{\partial \chi_L^{(3)}}{\partial w}\Big|_0 + \chi_2^{(3)} \frac{\partial v}{\partial w}\Big|_0 + v_0 \chi_2^{(3)} \left(1 - \frac{4}{n^2 + 2} \frac{\partial n^2}{\partial w}\Big|_0\right) = \frac{1}{M_1}\left(\frac{n^2 + 2}{3}\right)^4 N_A \gamma_1 \tag{14}$$

where M_1 is the solute molecular weight, $\chi_2^{(3)}$ the macroscopic third harmonic susceptibility of the solvent, N_A Avagadro's number and the subscript 0 denotes the infinite dilution limit. At 1907 nm, using the DMF values given in Section 3, the slope in Figure 4 and the measured value for $\frac{\partial n^2}{\partial w}$ of 0.72 ± 0.30 determined using a Fabry-Perot interferometer, γ_1, which is the isotropically averaged value $\langle\gamma\rangle$ for SINC, is found to be $-3140 \pm 250 \times 10^{-36}$ esu. THG measurements at shorter wavelengths show that at 1543 nm $\chi_L^{(3)}$ is independent of the SINC concentration, and, therefore, $\langle\gamma\rangle$ is less than the experimental uncertainty of $\pm 50 \times 10^{-36}$ esu. For a fundamental wavelength of 1064 nm, the absorption of the SINC solution at the third harmonic wavelength is too large for Maker fringes to be discernible.

We have previously[1,6] described in detail the origins of the electronic ground state $\gamma_{ijkl}(-\omega_4\omega_1,\omega_2,\omega_3)$ in strongly electron correlated conjugated 1D and 2D π-electron systems and illustrated the important virtual excitation processes that lead to their large nonresonant nonlinear optical susceptibilities. In the fully nonresonant case, where all optical frequencies are below electronic resonances, there are two major types of contributing terms to $\gamma_{ijkl}(-\omega_4;\omega_1,\omega_2,\omega_3)$. One of these, denoted type I, involves only the ground state and the dominant one-photon state and is negative definite. The other, type II, additionally involves a high-lying two-photon state and is positive definite. The latter term is slightly larger leading to a

$\gamma_{ijkl}(-\omega_4;\omega_1,\omega_2,\omega_3)$ that is positive in sign for frequencies below any resonances. We further found that, as a general rule, 2D conjugated structures have smaller nonresonant $\gamma_{ijkl}(-\omega_4;\omega_1,\omega_2,\omega_3)$ values than their 1D analogs since the effective length over which π-electrons can respond to the optical electric field is one-half the circumference for 2D structures as opposed to the full end-to-end length across the conjugation axis for 1D structures.

$\gamma_{ijkl}(-3\omega;\omega,\omega,\omega)$ of SINC can be understood in terms of the key examples of type I and type II third order virtual excitation processes schematically illustrated in Figure 5. The state S_n is a postulated large cross-section singlet state accessible through S_1 and S_2. The $S_0 \rightarrow S_1 \rightarrow S_0 \rightarrow S_1 \rightarrow S_0$ virtual excitation process shown in (a) is a type I term deriving from the large oscillator strength $S_0 \rightarrow S_1$ Q band excitation. A dominant type II term is shown in (b) where the $S_0 \rightarrow S_1 \rightarrow S_n \rightarrow S_1 \rightarrow S_0$ virtual excitation process involves both the $S_0 \rightarrow S_1$ and $S_1 \rightarrow S_n$ virtual transitions. Correspondingly, less important type I and type II virtual processes are illustrated in (c) and (d), respectively, where each involves the $S_0 \rightarrow S_2$ transition. Since the $S_0 \rightarrow S_1$ transition is much stronger than the $S_0 \rightarrow S_2$ transition, the virtual excitation processes shown in (a) and (b) dominate those shown in (c) and (d).

For the fundamental laser frequencies used in the present experiment of SINC in DMF, the third harmonic frequencies are larger than the Q band excitation energy at 1.59 eV. The 3ω resonance of the Q band occurs for a fundamental frequency that is one-third of the Q band excitation energy or 0.53 eV (2334 nm), and the 3ω resonance of the 3.70 eV B band occurs for a fundamental frequency of 1.23 eV (1005 nm). Since 1907 nm is above the 3ω resonance at 2334 nm, the

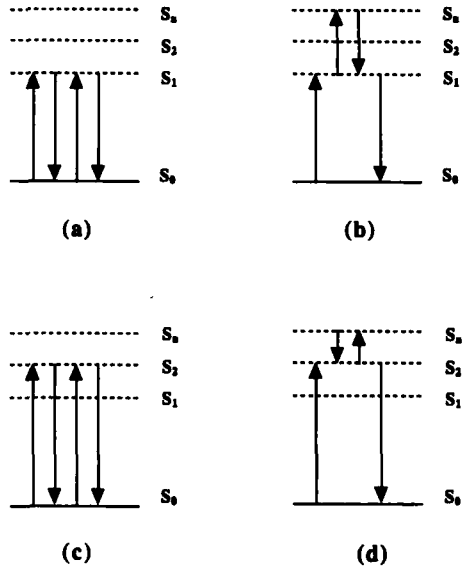

FIGURE 5 Key examples of third order virtual excitation processes contributing to $\gamma_{ijkl}(-3\omega;\omega,\omega,\omega)$ of SINC. The (a) type I and (b) type II virtual excitation processes that involve the $S_0 \rightarrow S_1$ virtual transition dominate the (c) type I and (d) type II processes that involve the $S_0 \rightarrow S_2$ transition.

experimentally measured value of $<\gamma>$ is negative for that fundamental wavelength. The close proximity of 1907 nm to 2334 nm also implies that $<\gamma>$ is near resonantly enhanced and, therefore, large in magnitude. The fundamental wavelength of 1543 nm, however, is well between the 3ω resonances of the Q and B bands, and the experimental value is very small since it lies in the crossover region between these resonances.

5. CONCLUSION

The isotropically averaged microscopic third harmonic susceptibility $<\gamma>$ has been measured for SINC in DMF at several nonresonant near infrared fundamental wavelengths. These measurements are complementary to earlier resonant studies of saturable absorption and absorptive optical bistability of SINC in random polymer films. In order to account for solute-solute and solvent-solvent interactions, an infinite dilution extrapolation method was presented that employs the third harmonic generation Maker fringe technique in the wedge configuration. At a fundamental wavelength of 1907 nm, $<\gamma>$ was measured to be $-3140 \pm 250 \times 10^{-36}$ esu, while at 1543 nm, $<\gamma>$ was less than the experimental sensitivity of $\pm 50 \times 10^{-36}$ esu. All the measured wavelengths lie between the 3ω resonances of the SINC Q and B absorption bands, but the large and negative $<\gamma>$ measured at 1907 nm is understood to result from near resonant enhancement due to the close proximity of this wavelength to the Q band 3ω resonance. In contrast, 1543 nm lies in the crossover region between the Q and B band 3ω resonances leading to a very small $<\gamma>$. These results illustrate the important effects of dispersion on $\gamma_{ijkl}(-\omega_4;\omega_1,\omega_2,\omega_3)$ of 1D and 2D conjugated molecular structures, even for near infrared wavelengths.

Acknowledgments

This research was generously supported by AFOSR and DARPA (grant F49621-85-C-0105), Penn Research Fund, and partially by NSF/MRL (grant DMR-85-19059). We gratefully acknowledge discussions with Dr. K. Y. Wong and the generous SINC sample supply from Drs. P. Kalyanaraman and J. Sounik of Hoechst-Celanese.

References

1. J. R. Heflin, K. Y. Wong, O. Zamani-Khamiri and A. F. Garito, *Phys. Rev.*, **B38**, 1573 (1988); and in Nonlinear Optical Properties of Polymers, A. J. Heeger, D. Ulrich and J. Orenstein, eds. (*Mater. Res. Soc. Proc.*, **109**, Pittsburgh, PA, 1988), pp. 91–102.
2. Z. G. Soos and S. Ramasesha, *Chem. Phys. Lett.*, **153**, 171 (1988); *J. Chem. Phys.*, **90**, 1067 (1989).
3. B. M. Pierce, *J. Chem. Phys.*, **91**, 791 (1989).
4. Z. Z. Ho, C. Y. Ju and W. M. Heatherington, *J. Appl. Phys.*, **62**, 716 (1987).
5. J. W. Wu, R. A. Norwood, J. R. Heflin, K. Y. Wong, O. Zamani-Khamiri and A. F. Garito, Topical Meeting on Nonlinear Optical Properties of Materials, 1988 Technical Digest Series. Vol. **9** (Optical Society of America, Washington, D.C., 1988), pp. 28–31.
6. J. W. Wu, J. R. Heflin, R. A. Norwood, K. Y. Wong, O. Zamani-Khamiri, A. F. Garito, P. Kalyanaraman and J. Sounik, *J. Opt. Soc. Am.*, **B6**, 707 (1989).

7. A. F. Garito and J. W. Wu, *Proc. SPIE*, **1147**, 2 (1990).
8. P. N. Prasad, M. K. Casstevens, J. Pfleger and P. Logadon, *Proc. SPIE*, **878**, 106 (1988).
9. J. S. Shirk, J. R. Lindle, F. J. Bartoli, C. A. Hoffman, Z. H. Zafafi and A. W. Snow, *Appl. Phys. Lett.*, **55**, 1287 (1989).
10. M. Hosoda, T. Wada, A. Yamada, A. F. Garito and H. Sasabe in *Multifunctional Materials*, ed. D. Ulrich, MRS Symp. Proc. Vol. **175** in press.
11. B. L. Wheeler, G. Nagasubramanian, A. J. Bard, L. A. Schectman, D. R. Dininny and M. E. Kenney, *J. Am. Chem. Soc.*, **106**, 7404 (1984).
12. See, for example, M. Gouterman, in *The Porphyrins*, ed. D. Dolphin (Academic, New York, 1978), Vol. **3**, Chap. 1.
13. W. F. Kosonocky and S. E. Harrison, *J. Appl. Phys.*, **37**, 4789 (1966).
14. F. Kajzar and J. Messier, *Rev. Sci. Instrum.*, **58**, 2081 (1987).
15. K. D. Singer and A. F. Garito, *J. Chem. Phys.*, **75**, 3572 (1981).
16. C. C. Teng and A. F. Garito, *Phys. Rev. Lett.*, **50**, 350 (1983) and *Phys. Rev.*, **B28**, 6766 (1983).
17. K. D. Singer, M. S. Merlin, C. H. Grossman and A. F. Garito, *Rev. Sci. Inst.*, **54**, 97 (1983).
18. G. R. Meredith, B. Buchalter and C. Hanzlik, *J. Chem. Phys.*, **78**, 1543 (1983).
19. F. Kajzar and J. Messier, *Phys. Rev.*, **A32**, 2352 (1985).